THE JOURNAL OF PHYSICAL CHEMISTRY C

Subscriber access provided by University of East Anglia Library

C: Physical Processes in Nanomaterials and Nanostructures

Time-Resolved Structural Dynamics of Extended #-Electron Porphyrin Nanoring

Giovanni Bressan, Martin D. Peeks, Harry L. Anderson, Stephen R. Meech, and Ismael Heisler

J. Phys. Chem. C, **Just Accepted Manuscript** • DOI: 10.1021/acs.jpcc.9b07494 • Publication Date (Web): 15 Oct 2019

Time-Resolved Structural Dynamics of Extended π-Electron Porphyrin Nanoring

Giovanni Bressan[1], Martin D. Peeks[2], Harry L. Anderson,[2] Stephen R. Meech[1] and Ismael A. Heisler[3,*]

[1]*School of Chemistry, Norwich Research Park, University of East Anglia, Norwich NR4 7TJ, United Kingdom*

[2]*Department of Chemistry, University of Oxford, Chemistry Research Laboratory, Oxford OX1 3TA, United Kingdom*

[3]*Departamento de Física, Universidade Federal do Paraná, Caixa Postal 19044, 81531-990 Curitiba, Parana, Brazil*

*Corresponding author. Email: heisler@fisica.ufpr.br

Abstract

Molecular structure design inspired by naturally occurring light harvesting systems has been intensely pursued over the last couple of decades. Interesting new structures include the π-conjugated porphyrin nanorings, which show promising features such as ultrafast excited-state delocalization, leading to suppressed radiative rates, superradiance with increasing temperature and energy transfer times comparable to their natural counterparts. An important question to be addressed in such systems is the role and time scale of structural motions and how they affect excited-state delocalization. Here it is shown that porphyrin nanorings which are not rigidified by a template are structurally heterogeneous in the ground state and evolve dynamically on a tens of picoseconds timescale. In the excited state a structural relaxation of the porphyrin nanorings is observed, on a picosecond timescale. Furthermore ultrafast excitation delocalization is observed, by anisotropy measurements, being insensitive to structural motions of the nanorings.

TOC graphics

Introduction

Molecular structures based on π-conjugated chromophores present attractive features such as semiconducting character[1,2,3] and nonlinear optical properties[4,5,6,7]. Various applications rely on such features including electroluminescent devices[8,9], solar cells[10,11], optical switches[12,13], and fluorescent biosensors[14,15]. The synthesis of conjugated porphyrin multi-chromophore structures tailored for specific applications has witnessed great progress during the last couple of decades[16,17]. A significant amount of work has been done on π-conjugated molecular systems comprised of extended linear one-dimensional oligomers[18,19,20], for which their physical properties correlate well with the length of the conjugated chain[21]. However, due to their finite size, linear oligomers present end-effects that can alter their physical behaviour[7,22,23]. These effects can be overcome by working with shape persistent and cyclically conjugated two-dimensional macrocycles. Such structures can behave like idealized, infinite π-conjugated oligomers with completely new photophysical characteristics[24,25]. Significantly, nature exploits such structures to harvest sunlight[26,27]. A number of photosynthetic organisms have evolved to use a wide variety of macrocycles comprising π-conjugated units to efficiently harvest solar energy and transfer it to reaction centers.[28,29]

Therefore, there is great interest in understanding the photophysics and excited state dynamics of conjugated nanorings. Excitations in such structures tend to exhibit highly delocalized character[25]. However, large extended chromophoric structures inevitably present conformational heterogeneity that can act as a perturbation and localize the excitation on a given chromophore or region of the macrocycle[30]. This is detrimental to the efficient operation envisaged for photonic structures and biomimetic light harvesting applications. An essential source of perturbation is provided by linking groups that affect and modulate the dihedral angle formed between the ring chromophoric units. The dihedral angle minimization (also called

"planarization") enhances the conjugation length, generally increasing excitation delocalization along the porphyrin oligomer structure.

The most important physical and chemical properties of π-conjugated chromophores involve their excited electronic states. However, excited states have relatively short lifetimes and therefore it is necessary to apply time resolved spectroscopy to infer detailed information about their photophysical and photochemical processes. Furthermore, given the high energy content in visible electronic excitation, structural motions can significantly affect the dynamics in π-conjugated chromophores and a better understanding of how such motions are coupled to electronic transitions is of great interest.

In this work we present a detailed study of ultrafast excited state dynamics of π-conjugated six-membered porphyrin nanorings, with (*c*-P6•T6) and without (*c*-P6) a template. The molecular structure of such compounds, together with a parent porphyrin dimer (P2) is shown in Figure 1. The aim is to investigate and characterize structural heterogeneity by monitoring changes in the electronic spectra. Ultrafast excitation delocalization and picosecond-timescale structural dynamics are revealed.

Experimental and Theoretical Methods

The time resolved measurements have been carried out on a conventional ultrafast transient absorption apparatus[31]. Briefly, an amplified Ti:Sapphire laser system (Spectra Physics Spitfire ACE), that generates 120 fs pulses centred at 800 nm with a repetition rate of 1 kHz, drives a commercial noncollinear optical parametric amplifier (NOPA, Light Conversion, TOPAS White), producing pulses around 20 fs duration, and also two collinear commercial OPAs (Light Conversion, TOPAS Prime) capable of giving 75 fs pulses tuneable from the UV to the IR. The NOPA pulses, used as pump, were recompressed close to the Fourier transform limit at the sample position and characterized by transient grating frequency resolved optical gating (TG-FROG) using a 1 mm fused silica window as the nonlinear medium. To generate broadband

probe pulses in the vis - near IR region, a 30 mm focal length lens was used to focus around 10 μJ, originating from an OPA centred at 1200 nm, onto a 3 mm thick sapphire window, to generate a supercontinuum spectrum spanning a spectral region from 550 nm until 1200 nm. Reflective optics were used (predominantly) in the experiment to direct the pump and probe pulses to the sample position, thus keeping the dispersion as low as possible. The pump and probe pulses were focused to spots with FWHM of 158 ± 7 μm and 37 ± 2 μm. The probe beam had its polarization set at 45° with regards to the pump beam. After the sample, the probe beam is split into two with a polarizing beam splitter and each polarization is measured simultaneously. The spectrum of both probe polarizations are measured at 1 kHz using two back-thinned full frame transfer (FFT) CCD cameras (Entwicklungsbuero Stresing) incorporated into a home-built two-channel prism-based spectrometer. An optical chopper was used to modulate the pump pulses at 500 Hz allowing transient absorption difference spectra to be calculated for consecutive probe pulses. The isotropic response is determined by calculating $S_{iso} = 1/3(S_{\parallel} + 2S_{\perp})$ whereas the anisotropy[31] is given by $S_{aniso} = (S_{\parallel} - S_{\perp})/(S_{\parallel} + 2S_{\perp})$.

The porphyrin nanorings were synthesised as reported previously[32,33] and dissolved in toluene with 1% v/v pyridine to prevent aggregation. The resulting solutions were placed in 1 mm optical path static cells for both the steady-state and time-resolved measurements, adjusting their concentration in order to obtain OD around 0.3 at their steady-state maxima. Measurements performed at lower concentration gave the same results, confirming that no aggregation was present.

Results and Discussion

The porphyrin structures studied here consist of nanorings composed by six meso-substituted zinc porphyrin units (aryl groups (3,5-bis(trihexylsilyl)benzene) at meso-positions) forming a circular structure through butadiyne links. Their structures are shown in Figure 1. The circular structure can be rigidified by the support of an inner hexapyridyl template (shown

in blue in Figure 1). Importantly, the butadiyne interconnecting links ensure complete π-conjugation of the nanoring, as evidenced by a large red shift of the lowest singlet absorption band (Q-band) relative to that of the bisalkynylporphyrin monomer[34]. The visible to near UV absorption spectrum of *c*-P6 and *c*-P6•T6 with their respective band assignments are shown in Figure S1. Similarly to other substituted porphyrin structures[34], the lowest energy spectral amplitude is related to transitions from the ground state into the so-called Q-band. Due to the asymmetric substitution present in the nanoring porphyrin units, the degeneracy of the transition dipole moments along the *x* and *y* axes is lifted[35].

Determination of the lowest energy transition of the nanoring structure is complicated. Nanoring systems, including the light-harvesting LH2 system, have a circular symmetry. Therefore, by analogy, the excited state energy-levels can be conveniently described by the Hückel molecular orbital theory for π-conjugated molecules.[36] The main outcome of the model is that there will be two nondegenerate k = 0 (S_1) and k = 3 (S_4) as well as two pairwise degenerate k = ±1 (S_2) and k = ±2 (S_3) electronic excited states. Furthermore, Hückel theory also indicates that only transition dipole moments to the two degenerate k = ±1 (S_2) states of orthogonal polarization (*x* and *y* transitions) carry significant oscillator strength. Additionally, according to the Kasha model, for a circular structure the transition dipole moment contributions will sum to zero, i.e., the lowest k = 0 (S_1) has a transition dipole moment strength equal to zero.[32] Once the molecule has relaxed into its lowest energy state, emission is expected to be strongly suppressed compared to the emission observed in the porphyrin monomer. This was indeed reported for *c*-P6 and *c*-P6•T6[33], which present a small fluorescence quantum yield (0.43% and 0.12%, respectively) and small radiative rate constants (0.029 ns^{-1} and 0.0048 ns^{-1} respectively). Thus, the intense absorption spectrum is assigned to the strongly allowed S_0 –> S_2 transition followed by a fast internal conversion to the S_1 state, where emission is suppressed. Given that *c*-P6 is not held in place by the template, it has some flexibility, so cancellation of

the transition dipoles is expected to be less complete, explaining a larger transition moment than for *c*-P6•T6.[25]

The dark state nature of the lowest excited singlet state in nanorings, makes the identification of the ground to first excited state (S_0 –> S_1) transition difficult. Recently time dependent density functional theory (TDDFT) estimated this transition to be at ~ 945 nm.[33] A further challenge remains the assignment of the sequence of similarly-spaced strong absorption peaks clearly visible in the templated nanoring *c*-P6•T6, at 777, 813, and 858 nm (Figure S1). One assignment was made in terms of a Franck−Condon progression of a vibrational mode coupled to the electronic transition[33], with a wavenumber around ~605 cm^{-1}. An alternative interpretation assigns electronic states to the peaks that appear in the absorption spectrum. This assignment was based on two-dimensional electronic spectroscopy measurements[37], where the analysis and classification of coherences of different origins allowed for the identification of electronic transitions present in these nanorings. However, an unambiguous and complete assignment of the origin of the peaks appearing in the absorption and emission spectra remains an elusive question.

A series of time-resolved pump-probe spectra for *c*-P6 and for *c*-P6•T6 are shown in Figures 2a and 2c (main graphs), together with the linear absorption and pump laser spectra (top graphs, shown in red and blue, respectively). For both structures the pump-probe signal consists of a strong ground state bleach (GSB) (680 nm – 890 nm, related to S_0 –> S_2 transitions) and a broad excited state absorption (ESA) which extends into the IR region as well as to wavelengths shorter than 680 nm. Those signals are established within the time resolution of our experiment (~50 fs) as can be seen in Figures 2b and 2d, an important observation indicating that the S_2 –> S_1 internal conversion is very efficient, as was also observed for other cyclic structures. Theoretical calculations performed on conjugated cycloparaphenylenes, made up of 14 monomers, have shown that the internal energy transfer to the lowest singlet excited state

happens on a 50 fs timescale[38]. The results presented on Figure 2b and 2d give evidence that such fast internal conversion also occurs for the porphyrin nanorings. There is no risetime or fast decay time observable for the ESA contribution, which would indicate any S_1 population formation or S_2 relaxation. Therefore, this process must be occurring during pulse overlap around time zero or on a timescale which is too fast to be resolved with our experimental setup.

As the inset of figures 2c and 2d shows, the ESA signal fully relaxes in a couple of nanoseconds whereas the GSB does not completely recover within the time range of our experiment. This can be assigned to triplet state formation, which relaxes back to the ground state over much longer timescales. The nonradiative rate constant for *c*-P6•T6 (k_{nr} = 1.6 ns^{-1}) is smaller than for *c*-P6 (k_{nr} = 2.03 ns^{-1}) and, therefore, the efficiency in accumulating population in the triplet state is reduced, producing a smaller offset in the final bleach values. Apart from a long time decay, there is a fast spectral evolution, mainly in the 820 – 1100 nm spectral region, during the first 500 fs, which is observed in both structures.

To quantify the time evolution of the whole pump-probe signal, we applied a global analysis fitting procedure to the data.[39] The resulting decay associated difference spectra (DADS) are shown in Figure 3 (normalized DADS are presented in Figure S6). To access quality of the fitting, time resolved curves at specific wavelengths together with fit are presented in Figure S2. For *c*-P6•T6 at least three components were necessary to completely fit the data whereas for *c*-P6 one additional time component was necessary. The shortest component, with a time constant around 150 fs, accounts for a fast spectral evolution already mentioned (in the region of the 820 – 1100 nm). This contribution can be assigned either to excited state energy equilibration within the vibronic energy levels or downhill vibrational energy relaxation. The much slower contributions are due to ESA decay and GSB recovery (462 ps for *c*-P6 and 241 ps for *c*-P6•T6) and triplet state formation (~ ns) that is not resolved in our experiment. The triplet states of *c*-P6 and *c*-P6•T6 have previously been observed with transient electron

paramagnetic resonance (EPR) spectroscopy by Tait et al[40], where they had lifetimes of hundreds of microseconds (at 20 K) and were fully delocalized on the EPR timescale. Furthermore, the longer relaxation time for *c*-P6 (462 ps) compared to *c*-P6•T6 (241 ps) can be explained by the fact that structural inhomogeneity breaks perfect circular symmetry of the *c*-P6 rings enabling slight increase in transition dipole moment. This is reflected in the higher radiative rate for *c*-P6 (0.029 ns^{-1}) when compared to *c*-P6•T6 (0.0048 ns^{-1}). An extra component, with a time constant of 200 ps, is required to describe the spectral evolution of *c*-P6. This component can be assigned to the molecular planarization in the excited state, i.e., minimization of the dihedral angles between the porphyrin monomers composing the nanoring as reported before.[41,42,43] Figure 4 compares curves at 900 nm and 910 nm (these wavelengths were chosen because the rising signal is maximized at those specific wavelengths), corresponding to ESA, for *c*-P6 and *c*-P6•T6, respectively, clearly evidencing the absence of a rising ESA signal for *c*-P6•T6. This is so because the *c*-P6•T6 structure is rigidified by the support of an inner hexapyridyl template, which keeps the porphyrin rings planarized. Furthermore, in the same figure, a comparison is made with a measurement done for the *c*-P6 parent dimer, P2, for which the planarization in the excited state was already well characterized[44]. The curves for *c*-P6 and P2 overlap almost perfectly, providing strong evidence for the origin of this contribution to the pump-probe signal.

Further evidence for the structural inhomogeneity present in the *c*-P6 solution is provided in Figure 5. A comparison is made between pump-probe curves obtained when exciting *c*-P6 at high energy (pump centred at 720 nm, blue curve) with excitation of *c*-P6 set at a low energy (pump centre at 850 nm, red curve). Figure 4, corresponding to an early time (T = 100 fs) transient spectra, shows that when excitation is set at low energy, the transient absorption shows the well resolved peaks as for the rigidified *c*-P6•T6 structure. Whereas for the same early times, when excitation is set at higher energies, a much smoother transient spectrum is obtained. The

explanation proposed for this is that *c*-P6 within the solution has a considerable amount of static disorder, caused by the distribution of dihedral angles between the porphyrin units that make up the nanoring. This assignment is confirmed by comparison to an equivalent set of measurements performed on templated *c*-P6•T6, as shown in Figure S3. For *c*-P6•T6, the spectral shape of pump-probe spectra is independent from excitation Structures which have, on average, larger dihedral angles present higher transition energies whereas structures with smaller dihedral angles[42,45], i.e., more planarized, will have smaller transition energies. Thus excitation at lower energies will give transient spectra resembling more *c*-P6•T6, in which the dihedral angles are kept fixed at small values by the hexapyridyl inner template. The transient behaviour is in agreement with what is observed for *c*-P6 and *c*-P6•T6 linear absorption spectra, where the rigidified structure *c*-P6•T6, which has small dihedral angles between its comprising porphyrin units, absorbs at lower energies when compared to the non-templated *c*-P6 nanoring. Therefore, what Figure 5a shows is that the low energy excitation preferentially excites the planarized structures among the distribution. In other words, changing the wavelength of the excitation pulse, selective excitation (hole-burning) of different subsets of nanorings is performed, with a relatively narrow distribution of dihedral angles (more twisted on the blue side and more planar on the red side) among the inhomogeneously broadened distribution of *c*-P6 nanorings in solution.

As time evolves, there is a dynamical evolution of the structures and the dihedral angles can change, altering the distribution's absorption spectrum. This is shown in Figure 5b and 5c. As the delay time between pump and probe increases, the peaks start to be "washed out", resulting in transient spectra for different excitations to become very similar. The time constant retrieved for this dihedral angle randomization in the ground state (given that the GSB is being observed) is 55 ps. This time constant is obtained by fitting the residual of the difference between pump-probe curves obtained when exciting *c*-P6 at high energy (pump centred at 720nm) with

excitation of *c*-P6 set at a low energy (pump centre at 850nm) (Figure S4). Therefore, this process is almost 4 times faster than the excited state planarization. Interestingly, the planarization in the excited state of the untemplated ring is almost four times slower than the random fluctuations taking place in its ground state. This is in contrast to what was observed in the parent dimer P2, in which structural dynamics occurs on a slower timescale in the ground state. These differences are related to the nature of the electronic excited states in which electronic dynamics are taking place, with the S_1 excited state of P2 resembling more S_2 of *c*-P6, which is initially populated. Due to the ultrafast S_2 -> S_1 population transfer in *c*-P6, planarization takes place in S_1 which has a different character than S_1 state in P2.

Finally, the wavelength and time resolved anisotropy was determined, as shown for *c*-P6 in Figure 6a and for *c*-P6•T6 in Figure S5. The two-dimensional plot shows the anisotropy as a colour scale for a given wavelength and time. The top graph shows the laser spectrum (blue), steady-state absorption spectrum (red) and an isotropic transient absorption curve at T=200fs (green). When the isotropic signal crosses zero the anisotropy becomes undefined (at around 675 and 900 nm). The main feature of this graph is that there is no major anisotropy variation across the spectral region studied. The anisotropy value is around 0.1, apart from very early times. This is so for *c*-P6 (Figure 6a) and for *c*-P6•T6 (Figure S5), implying that anisotropy is not affected by structural inhomogeneity. Figure 6b shows the anisotropy time evolution for a wavelength equal to 1050 nm, located in the ESA region. It is possible to resolve a fast (~ 50 fs) decay during the first 200 fs, after which the anisotropy value stabilizes at around 0.1. As the inset graph shows, this value persists until the excited state signal has fully relaxed, even for *c*-P6. An anisotropy value of 0.1 is expected for a system which has no preferred excitation polarization direction as well no preferred emission dipole moment. This is exactly the case for transitions in the nanoring plane, where the polarization memory is completely lost in a two-dimensional plane. However, energy transfer among the ring chromophores could also lead to

this randomization, it is however unlikely. It would have to be extremely fast given that it has to cover a distance of ~ 15 nm (circumference length of a 2.4 nm ring) in 50 fs.

Wynne and Hochstrasser have shown[46] that, when exciting degenerate states that have their transition dipole moment orthogonal, the electronic coherence properties of the two states involved need to be considered. In such a case the anisotropy value can be as high as 0.7 but quickly decays to a value of 0.1 as the coherence between states is lost. Therefore, the fast 50 fs decay measured here, which is within the instrument time resolution, indicates a decoherence between k = ±1 states. Importantly, it also indicates that the excitation delocalizes along the nanoring within this fast timescale. This result confirms the earlier suggestion[30] that both the absorbing and the emitting states must be fully delocalized over the nanoring.

Conclusions

The photophysics of two different π-electron porphyrin nanorings was investigated through time resolved pump-probe spectroscopy. The non-templated *c*-P6 nanoring shows significant structural dynamics. In the excited sate, planarization occurs on a time scale of 200 ps whereas in the ground state dihedral angle randomization occurs faster, with a timescale of 55 ps. On the other hand, the addition of an inner template, rigidifies the nanoring structure. Therefore, for *c*-P6•T6 no significant structural motions are observed. In both nanorings, ultrafast excited state delocalization occurs along the whole nanoring, as evidenced by anisotropy measurements. The delocalization is faster than 50 fs, the instrumental response function used in this work. Interestingly, the excitation remains delocalized for the whole excited state population time and is not affected by structural motions as present in *c*-P6.

Acknowledgments

This work was supported by EPSRC grants EP/J009148/1 and J021431/1.

Supporting Information

Additional figures including UV-Vis absorption, residual difference curve, *c*-P6•T6 anisotropy measurement.

Figure Captions

Figure 1. Porphyrin structures consist of nanorings composed by six meso-substituted zinc porphyrin units (bearing aryl groups (3,5-bis(trihexylsilyl)benzene) at meso-positions) forming a circular structure through butadiyne links**.** *c*-P6**•**T6 is the templated ring, *c*-P6 is the same structure without the hexapyridyl template (shown in blue). P2 is the parent dimer.

Figure 2. Transient absorption spectra at several probe delay times for (a) *c*-P6 and (c) *c*-P6**•**T6. Graphs (b) and (d) show time resolved transient absorption curves taken at selected probing wavelengths of 1083 (red) and 776 nm (blue) for *c*-P6 and 1100 (red) and 809 nm (blue) for *c*-P6**•**T6.

Figure 3. Decay associated difference spectra (DADS) for (a) *c*-P6 and (b) *c*-P6**•**T6.

Figure 4. Comparison of time resolved transient absorption curves taken at selected probing wavelengths: 900 nm for *c*-P6 (black), 910 nm for *c*-P6**•**T6 (red) and 1160 nm for P2 (blue). The right hand side scale is related only to the P2 (blue) curve.

Figure 5. Transient absorption spectra for *c*-P6 at two different excitation conditions, as shown in the top graph, centred at 700 nm (blue) and 830 nm (red). The different graphs correspond to different pump-probe delay times as for (a) T=0.1 ps, (b) T=10 ps and (c) T=120 ps.

Figure 6. (a) Two-dimensional plot showing the anisotropy as a colour scale. The top graph shows the laser spectrum (blue), absorption spectrum (red) and an isotropic transient absorption curve at T=200fs (green). (b) Anisotropy as a function of time taken at a selected probing wavelength of 1051 nm (black) and fit to the data (red).

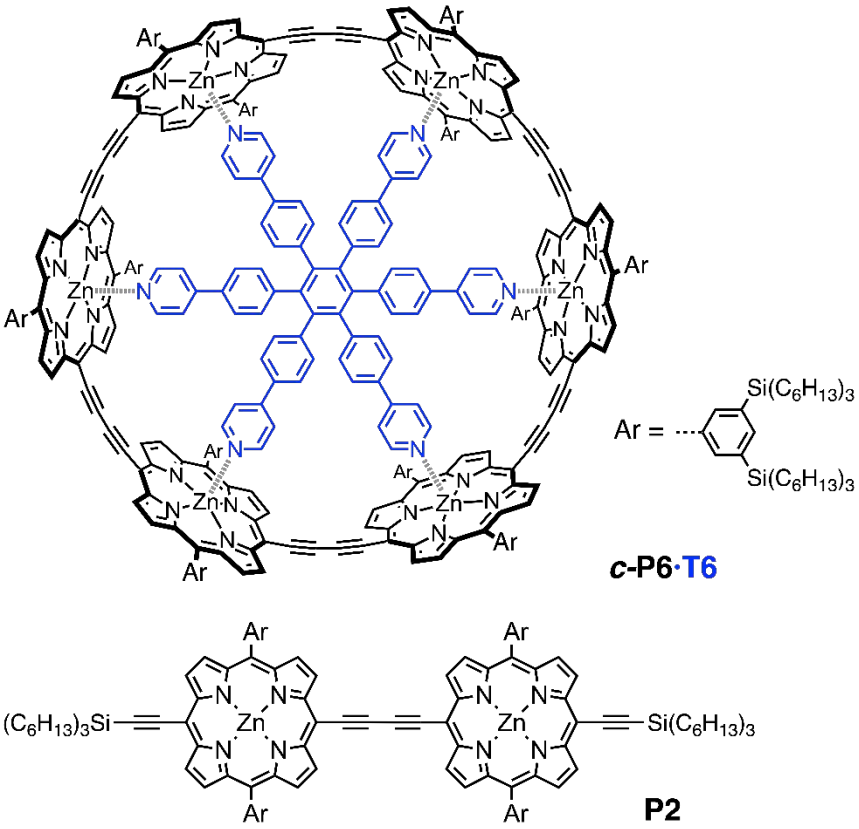

Figure 1

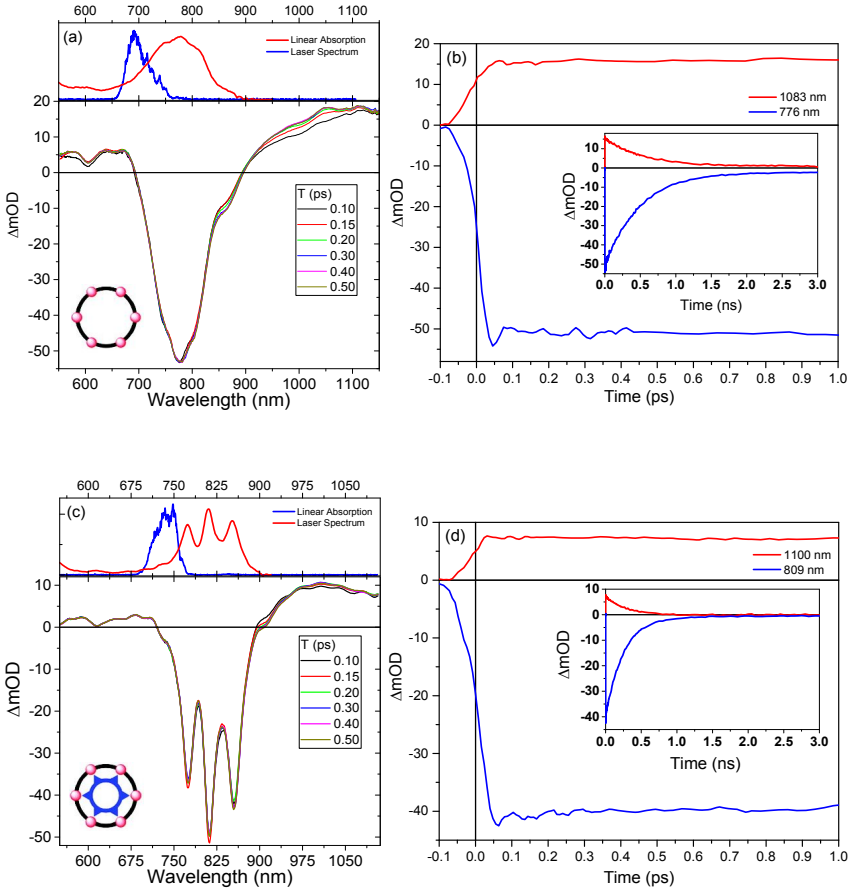
(a)
Linear Absorption
Laser Spectrum
T (ps)
0.10
0.15
0.20
0.30
0.40
0.50
ΔmOD
Wavelength (nm)
(b)
1083 nm
776 nm
ΔmOD
Time (ps)
Time (ns)
(c)
Linear Absorption
Laser Spectrum
T (ps)
0.10
0.15
0.20
0.30
0.40
0.50
ΔmOD
Wavelength (nm)
(d)
1100 nm
809 nm
ΔmOD
Time (ps)
Time (ns)

Figure 2

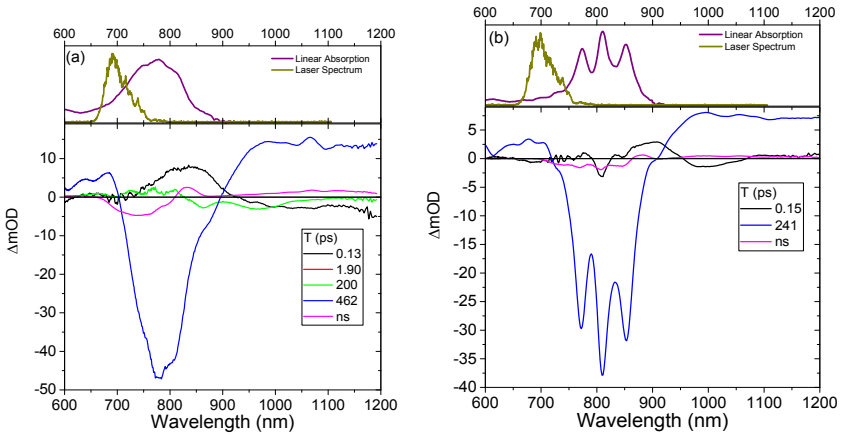
(a)
Linear Absorption
Laser Spectrum
T (ps)
0.13
1.90
200
462
ns
ΔmOD
Wavelength (nm)
(b)
Linear Absorption
Laser Spectrum
T (ps)
0.15
241
ns
ΔmOD
Wavelength (nm)

Figure 3

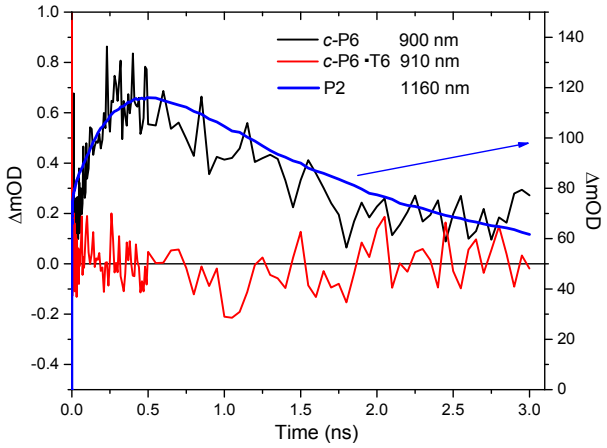
c-P6 900 nm
c-P6 •T6 910 nm
P2 1160 nm
ΔmOD
ΔmOD
Time (ns)
1.0
0.8
0.6
0.4
0.2
0.0
-0.2
-0.4
140
120
100
80
60
40
20
0
0.0
0.5
1.0
1.5
2.0
2.5
3.0

Figure 4

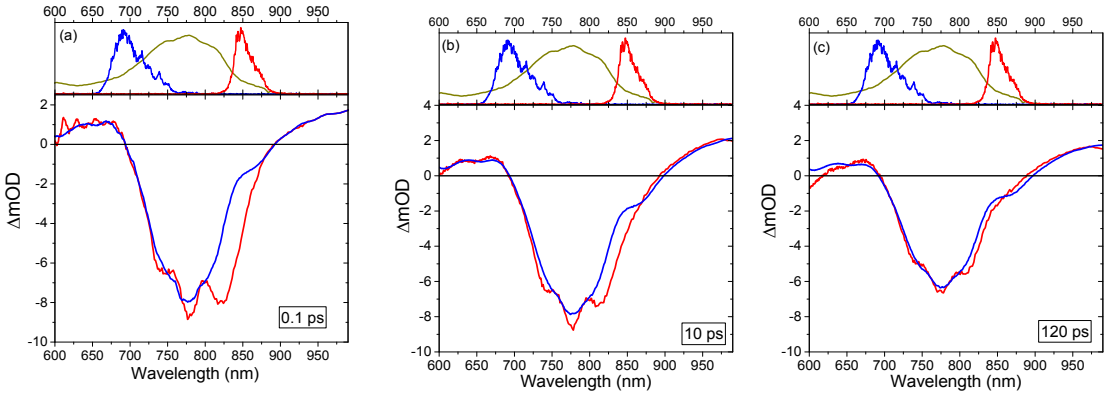

Figure 5

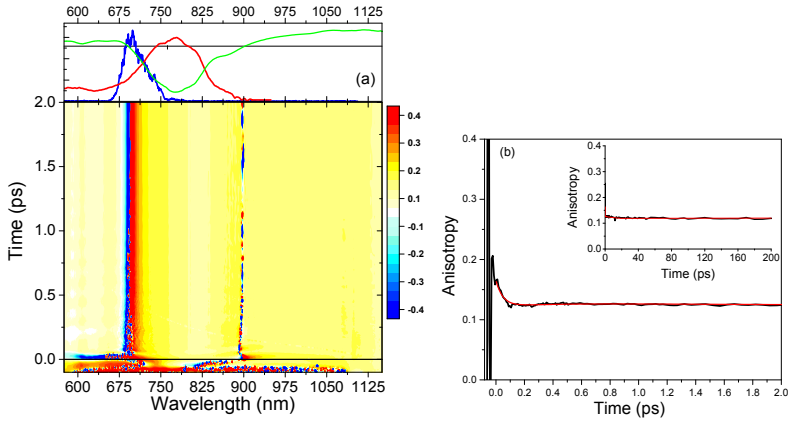

Figure 6

References

(1) Hafner, R. J.; Tian, L.; C. Brauer, J.; Schmaltz, T.; Sienkiewicz, A.; Balog, S.; Flauraud, V.; Brugger, J.; Frauenrath, H. Unusually Long-Lived Photocharges in Helical Organic Semiconductor Nanostructures. *ACS Nano* **2018**, *12* (9), 9116–9125.

(2) Huang, Y.; Xu, Z.; Jin, S.; Li, C.; Warncke, K.; A. Evangelista, F.; Lian, T.; Egap, E. Conjugated Oligomers with Stable Radical Substituents: Synthesis, Single Crystal Structures, Electronic Structure, and Excited State Dynamics. *Chem. Mater.* **2018**, *30* (21), 7840–7851.

(3) Walzer, K.; Maennig, B.; Pfeiffer, M.; Leo, K. Highly Efficient Organic Devices Based on Electrically Doped Transport Layers. *Chem. Rev.* **2007**, *107* (4), 1233–1271.

(4) McEwas, K. J.; Bourhill, G.; Robertson, J. M.; Anderson, H. L. The Nonlinear Optical Characterization Of Meso-Susbtituted Porphyrin Dyes. *J. Nonlinear Opt. Phys. Mater.* **2000**, *09* (04), 451–468.

(5) B. Teran, N.; S. He, G.; Baev, A.; Shi, Y.; T. Swihart, M.; N. Prasad, P.; J. Marks, T.; R. Reynolds, J. Twisted Thiophene-Based Chromophores with Enhanced Intramolecular Charge Transfer for Cooperative Amplification of Third-Order Optical Nonlinearity. *J. Am. Chem. Soc.* **2016**, *138* (22), 6975–6984.

(6) W. Becker, M.; S. Sapochak, L.; Ghosen, R.; Xu, C.; R. Dalton, L.; Shi, Y.; H. Steier, W.; K.-Y. Jen, A. Large and Stable Nonlinear Optical Effects Observed for a Polyimide Covalently Incorporating a Nonlinear Optical Chromophore. *Chem. Mater.* **2002**, *6* (2), 104–106.

(7) Ogawa, K.; Zhang, T.; Yoshihara, K.; Kobuke, Y. Large Third-Order Optical Nonlinearity of Self-Assembled Porphyrin Oligomers. *J. Am. Chem. Soc.* **2001**, *124* (1), 22–23.

(8) Qian, G.; Dai, B.; Luo, M.; Yu, D.; Zhan, J.; Zhang, Z.; Ma, D.; Yuan Wang, Z. Band Gap Tunable, Donor−Acceptor−Donor Charge-Transfer Heteroquinoid-Based Chromophores: Near Infrared Photoluminescence and Electroluminescence. *Chem. Mater.* **2008**, *20* (19), 6208–6216.

(9) Gankin, A.; Mervinetsky, E.; Alshanski, I.; Buchwald, J.; Dianat, A.; Gutierrez, R.; Cuniberti, G.; Sfez, R.; Yitzchaik, S. ITO Work Function Tunability by Polarizable Chromophore Monolayers. *Langmuir* **2019**, *35* (8), 2997–3004.

(10) Chandrabose, S.; Chen, K.; J. Barker, A.; J. Sutton, J.; K. K. Prasad, S.; Zhu, J.; Zhou, J.; C. Gordon, K.; Xie, Z.; Zhan, X.; et al. High Exciton Diffusion Coefficients in Fused Ring Electron Acceptor Films. *J. Am. Chem. Soc.* **2019**, *141* (17), 6922–6929.

(11) Kay, A.; Graetzel, M. Artificial Photosynthesis. 1. Photosensitization of Titania Solar Cells with Chlorophyll Derivatives and Related Natural Porphyrins. *J. Phys. Chem.* **2002**, *97* (23), 6272–6277.

(12) S. He, G.; Zhu, J.; Baev, A.; Samoć, M.; L. Frattarelli, D.; Watanabe, N.; Facchetti, A.; Ågren, H.; J. Marks, T.; N. Prasad, P. Twisted π-System Chromophores for All-Optical Switching. *J. Am. Chem. Soc.* **2011**, *133* (17), 6675–6680.

(13) Ambroise, A.; W. Wagner, R.; Dharma Rao, P.; A. Riggs, J.; Hascoat, P.; R. Diers, J.;

Seth, J.; K. Lammi, R.; F. Bocian, D.; Holten, D.; et al. Design and Synthesis of Porphyrin-Based Optoelectronic Gates. *Chem. Mater.* **2001**, *13* (3), 1023–1034.

(14) Rong, Y.; Wu, C.; Yu, J.; Zhang, X.; Ye, F.; Zeigler, M.; Elena Gallina, M.; Wu, I.-C.; Zhang, Y.; Chan, Y.-H.; et al. Multicolor Fluorescent Semiconducting Polymer Dots with Narrow Emissions and High Brightness. *ACS Nano* **2013**, *7* (1), 376–384.

(15) Wang, B.; Yu, C. Fluorescence Turn-on Detection of a Protein through the Reduced Aggregation of a Perylene Probe. *Angew. Chemie - Int. Ed.* **2010**, *49* (8), 1485–1488.

(16) J. M. Hoeben, F.; Jonkheijm, P.; W. Meijer, E.; P. H. J. Schenning, A. About Supramolecular Assemblies of π-Conjugated Systems. *Chem. Rev.* **2005**, *105* (4), 1491–1546.

(17) Bols, P. S.; Anderson, H. L. Template-Directed Synthesis of Molecular Nanorings and Cages. *Acc. Chem. Res.* **2018**, *51* (9), 2083–2092.

(18) Joong Lee, S.; T. Hupp, J.; T. Nguyen, S. Growth of Narrowly Dispersed Porphyrin Nanowires and Their Hierarchical Assembly into Macroscopic Columns. *J. Am. Chem. Soc.* **2008**, *130* (30), 9632–9633.

(19) Fathalla, M.; Neuberger, A.; Li, S.-C.; Schmehl, R.; Diebold, U.; Jayawickramarajah, J. Straightforward Self-Assembly of Porphyrin Nanowires in Water: Harnessing Adamantane/β-Cyclodextrin Interactions. *J. Am. Chem. Soc.* **2010**, *132* (29), 9966–9967.

(20) Bressan, G.; Green, D.; Chan, Y.; Bulman Page, P. C.; Jones, G. A.; Meech, S. R.; Heisler, I. A. One- to Two-Exciton Transitions in Perylene Bisimide Dimer Revealed by Two-Dimensional Electronic Spectroscopy. *J. Phys. Chem. A* **2019**, *123* (8), 1594–1601.

(21) Liu, X.; Sun, Y.; A. Perez, L.; Wen, W.; F. Toney, M.; J. Heeger, A.; C. Bazan, G. Narrow-Band-Gap Conjugated Chromophores with Extended Molecular Lengths. *J. Am. Chem. Soc.* **2012**, *134* (51), 20609–20612.

(22) Ma, W.; Yang, C.; Gong, X.; Lee, K.; Heeger, A. J. Thermally Stable, Efficient Polymer Solar Cells with Nanoscale Control of the Interpenetrating Network Morphology. *Adv. Funct. Mater.* **2005**, *15* (10), 1617–1622.

(23) Mena-Osteritz, E. Superstructures of Self-Organizing Thiophenes. *Adv. Mater.* **2002**, *14* (8), 609–616.

(24) Donehue, J. E.; Varnavski, O. P.; Cemborski, R.; Iyoda, M.; Goodson, T. Probing Coherence in Synthetic Cyclic Light-Harvesting Pigments. *J. Am. Chem. Soc.* **2011**, *133* (13), 4819–4828.

(25) Yong, C.-K.; Parkinson, P.; Kondratuk, D. V.; Chen, W.-H.; Stannard, A.; Summerfield, A.; Sprafke, J. K.; O'Sullivan, M. C.; Beton, P. H.; Anderson, H. L.; et al. Ultrafast Delocalization of Excitation in Synthetic Light-Harvesting Nanorings. *Chem. Sci.* **2015**, *6* (1), 181–189.

(26) McDermott, G.; Prince, S. M.; Freer, a. a.; Hawthornthwaite-Lawless, a. M.; Papiz, M. Z.; Cogdell, R. J.; Isaacs, N. W. Crystal Structure of an Integral Membrane Light-Harvesting Complex From Photosynthetic Bacteria. *Nature*. **1995**, *374*, 517–521.

(27) D. Scholes, G. Quantum-Coherent Electronic Energy Transfer: Did Nature Think of It First? *J. Phys. Chem. Lett.* **2010**, *1* (1), 2–8.

(28) Wang, L.; Allodi, M. A.; Engel, G. S. Quantum Coherences Reveal Excited-State Dynamics in Biophysical Systems. *Nat. Rev. Chem.* **2019**, *3*, 477–490.

(29) Kondo, T.; Jia Chen, W.; S. Schlau-Cohen, G. Single-Molecule Fluorescence Spectroscopy of Photosynthetic Systems. *Chem. Rev.* **2017**, *117* (2), 860–898.

(30) Parkinson, P.; Kondratuk, D. V.; Menelaou, C.; Gong, J. Q.; Anderson, H. L.; Herz, L. M. Chromophores in Molecular Nanorings: When Is a Ring a Ring? *J. Phys. Chem. Lett.* **2014**, *5* (24), 4356–4361.

(31) Berera, R.; van Grondelle, R.; Kennis, J. T. M. Ultrafast Transient Absorption Spectroscopy: Principles and Application to Photosynthetic Systems. *Photosynth. Res.* **2009**, *101* (2–3), 105–118.

(32) Hoffmann, M.; Kärnbratt, J.; Chang, M. H.; Herz, L. M.; Albinsson, B.; Anderson, H. L. Enhanced π-Conjugation around a Porphyrin[6] Nanoring. *Angew. Chemie - Int. Ed.* **2008**, *47* (27), 4993–4996.

(33) Sprafke, J. K.; Kondratuk, D. V.; Wykes, M.; Thompson, A. L.; Hoffmann, M.; Drevinskas, R.; Chen, W. H.; Yong, C. K.; Karnbratt, J.; Bullock, J. E.; et al. Belt-Shaped π-Systems: Relating Geometry to Electronic Structure in a Six-Porphyrin Nanoring. *J. Am. Chem. Soc.* **2011**, *133* (43), 17262–17273.

(34) V. A. Camargo, F.; L. Anderson, H.; R. Meech, S.; A. Heisler, I. Full Characterization of Vibrational Coherence in a Porphyrin Chromophore by Two-Dimensional Electronic Spectroscopy. *J. Phys. Chem. A* **2014**, *119* (1), 95–101.

(35) Anderson, H. L. Building Molecular Wires from the Colors of Life: Conjugated Porphyrin Oligomers. *Chem. Commun.*, **1999**, *23*, 2323-2330.

(36) Gong, J. Q.; Favereau, L.; Anderson, H. L.; Herz, L. M. Breaking the Symmetry in Molecular Nanorings. *J. Phys. Chem. Lett.* **2016**, *7* (2), 332–338.

(37) Butkus, V.; Alster, J.; Bašinskaite, E.; Augulis, R.; Neuhaus, P.; Valkunas, L.; Anderson, H. L.; Abramavicius, D.; Zigmantas, D. Discrimination of Diverse Coherences Allows Identification of Electronic Transitions of a Molecular Nanoring. *J. Phys. Chem. Lett.* **2017**, *8* (10), 2344–2349.

(38) Adamska, L.; Nayyar, I.; Chen, H.; Swan, A. K.; Oldani, N.; Fernandez-Alberti, S.; Golder, M. R.; Jasti, R.; Doorn, S. K.; Tretiak, S. Self-Trapping of Excitons, Violation of Condon Approximation, and Efficient Fluorescence in Conjugated Cycloparaphenylenes. *Nano Lett.* **2014**, *14* (11), 6539–6546.

(39) Snellenburg, J. J.; Laptenok, S. P.; Seger, R.; Mullen, K. M.; van Stokkum, I. H. M. Glotaran : A Java -Based Graphical User Interface for the R Package TIMP. *J. Stat. Softw.* **2012**, *49* (3), 1-10.

(40) Tait, C. E.; Neuhaus, P.; Peeks, M. D.; Anderson, H. L.; Timmel, C. R. Transient EPR Reveals Triplet State Delocalization in a Series of Cyclic and Linear π-Conjugated Porphyrin Oligomers. *J. Am. Chem. Soc.* **2015**, *137* (25), 8284–8293.

(41) Chang, M.-H.; Hoffmann, M.; L. Anderson, H.; M. Herz, L. Dynamics of Excited-State

Conformational Relaxation and Electronic Delocalization in Conjugated Porphyrin Oligomers. *J. Am. Chem. Soc.* **2008**, *130* (31), 10171–10178.

(42) U. Winters, M.; Kärnbratt, J.; Eng, M.; J. Wilson, C.; L. Anderson, H.; Albinsson, B. Photophysics of a Butadiyne-Linked Porphyrin Dimer: Influence of Conformational Flexibility in the Ground and First Singlet Excited State. *J. Phys. Chem. C* **2007**, *111* (19), 7192–7199.

(43) V. A. Camargo, F.; L. Anderson, H.; R. Meech, S.; A. Heisler, I. Time-Resolved Twisting Dynamics in a Porphyrin Dimer Characterized by Two-Dimensional Electronic Spectroscopy. *J. Phys. Chem. B* **2015**, *119* (46), 14660–14667.

(44) Camargo, F. V. A.; Hall, C. R.; Anderson, H. L.; Meech, S. R.; Heisler, I. A. Time Resolved Structural Dynamics of Butadiyne-Linked Porphyrin Dimers. *Struct. Dyn.* **2016**, *3* (2), 023608.

(45) Peeks, M. D.; Neuhaus, P.; Anderson, H. L. Experimental and Computational Evaluation of the Barrier to Torsional Rotation in a Butadiyne-Linked Porphyrin Dimer. *Phys. Chem. Chem. Phys.* **2016**, *18* (7), 5264–5274.

(46) Wynne, K.; Hochstrasser, R. M. Anisotropy as an Ultrafast Probe of Electronic Coherence in Degenerate Systems Exhibiting Raman Scattering, Fluorescence, Transient Absorption and Chemical Reactions. *J. Raman Spectrosc.* **1995**, *26* (7), 561–569.

TOC graphic: